Skewness of mean transverse momentum fluctuations in heavy-ion collisions

Giuliano Giacalone,[1] Fernando G. Gardim,[2] Jacquelyn Noronha-Hostler,[3] and Jean-Yves Ollitrault[1]

[1]*Université Paris Saclay, CNRS, CEA, Institut de physique théorique, 91191 Gif-sur-Yvette, France*
[2]*Instituto de Ciência e Tecnologia, Universidade Federal de Alfenas, 37715-400 Poços de Caldas, MG, Brazil*
[3]*Department of Physics, University of Illinois at Urbana-Champaign, Urbana, IL 61801, USA*

We propose the skewness of mean transverse momentum, $\langle p_t \rangle$, fluctuations as a fine probe of hydrodynamic behavior in relativistic nuclear collisions. We describe how the skewness of the $\langle p_t \rangle$ distribution can be analyzed experimentally, and we use hydrodynamic simulations to predict its value. We predict in particular that $\langle p_t \rangle$ fluctuations have positive and nontrivial skew at a given collision centrality. We elucidate the origin of this result by deriving generic formulas relating the fluctuations of $\langle p_t \rangle$ to the fluctuations of the early-time thermodynamic quantities. We thus argue that the positive skewness of $\langle p_t \rangle$ fluctuations is a universal prediction of hydrodynamic models.

I. INTRODUCTION

In ultrarelativistic nucleus-nucleus collisions, the mean transverse momentum, $\langle p_t \rangle$, of emitted particles fluctuates event to event, for a given collision centrality. There are trivial *statistical* fluctuations of $\langle p_t \rangle$, due to the fact that the average is evaluated over a finite sample of particles, but the observed fluctuations are larger. The excess fluctuations are called *dynamical* fluctuations, and have been measured in Au+Au collisions at $\sqrt{s_{\rm NN}} = 200$ GeV [1] and lower energies [2–4], and in Pb+Pb collisions at $\sqrt{s_{\rm NN}} = 2.76$ TeV [5]. Dynamical $\langle p_t \rangle$ fluctuations are thought to originate from event-to-event fluctuations at the early stage of the collision. Some hydrodynamic models of particle production, supplemented with the appropriate modeling of the initial stages, are able to reproduce experimental data on $\langle p_t \rangle$ fluctuations [6, 7].

In this paper, we argue that, at a given collision centrality, the probability distribution of $\langle p_t \rangle$ is not Gaussian, but has positive skew. In Sec. II we show that a hint of this positive skew can be seen in existing STAR data [2] on Au+Au collisions, while it is clearly visible in the results of event-by-event hydrodynamic simulations of Pb+Pb collisions. This constitutes a solid basis for investigating this phenomenon. We define measures of the skewness of $\langle p_t \rangle$ fluctuations in Sec. III, with detailed explanations about the analysis procedure to measure them given in Appendix A, and we make quantitative predictions for these quantities using hydrodynamic calculations in Sec. IV. The resulting skewness is positive, and also nontrivial, in the sense that it deviates from the expectation of trivial distributions with positive support.

We investigate, hence, the origin of the skewness. In Sec. V, we use the idea put forward in Refs. [8, 9] that the fluctuations of $\langle p_t \rangle$ at a given centrality originate from the fluctuations of the total energy in the fluid at the initial condition, E_0. We first show that the distribution of E_0 is indeed positively skewed in our hydrodynamic calculation, and then argue that this is a generic prediction of hydrodynamics, which does not depend on the specific setup used in this paper. This is done in Sec. VI, where we derive a generic formula relating the skewness of the

E_0 distribution to the statistical properties of the initial density field in a perturbative approach [10, 11].

II. SKEWNESS IN DATA AND IN HYDRODYNAMICS

Figure 1 displays the histogram of the distribution of $\langle p_t \rangle$ measured by the STAR collaboration in central Au+Au collisions [2], where $\langle p_t \rangle$ is evaluated by averaging the transverse momenta of the charged particles observed in the detector. As mentioned in the Introduction, this quantity has trivial fluctuations due to the finite number of particles, typically of order 1000, in every event. The width of the distribution of $\langle p_t \rangle$ is actually
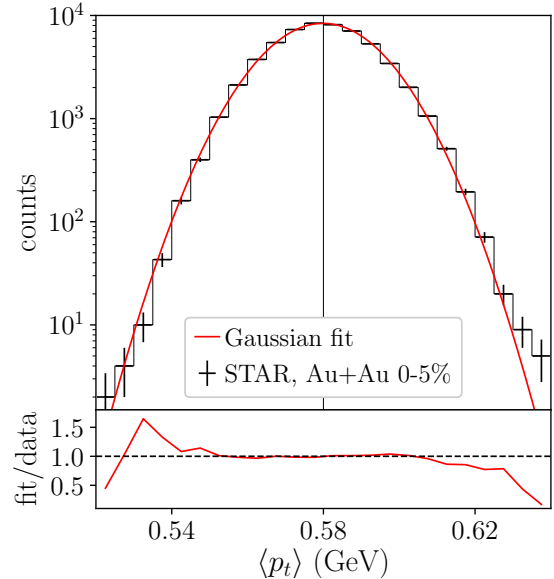

FIG. 1. (Color online) Distribution of $\langle p_t \rangle$ for Au+Au collisions at $\sqrt{s_{\rm NN}} = 200$ GeV in the 0-5% centrality window. Data from the STAR collaboration [2] are shown as a histogram. The solid line is a Gaussian fit to these data. The lower panel is the ratio between the Gaussian fit and the data. The data are above the Gaussian to the right, and below the Gaussian to the left, which hints at a positive skew.

dominated by these statistical fluctuations, and the dynamical fluctuations only represent a modest fraction of this width. Even though this histogram does not represent a distribution of dynamical fluctuations, it is instructive to see that the distribution is not symmetric. Comparison with a Gaussian fit, shown as a solid line, shows that the data points are above the fit to the right, and below the fit to the left, which is an indication that the distribution of $\langle p_t \rangle$ has positive skew.

We present now the distribution of $\langle p_t \rangle$ in event-by-event hydrodynamics.

The setup of our hydrodynamic calculation is the same as in Ref. [12]. 50000 minimum bias Pb+Pb collisions at $\sqrt{s_{\rm NN}} = 5.02$ TeV are evolved in 2+1 dimensions through the viscous hydrodynamic code V-USPHYDRO [13–15], starting from an initial profile of entropy density given, event-to-event, by the TRENTo model of initial conditions [16], which has been tuned following Ref. [17].[1] Events are sorted into centrality bins according to their total initial entropy (5% bins are used). This is done to mimic the centrality selection performed in experiments. We neglect the pre-equilibrium dynamics of the system [18–20], which is evolved hydrodynamically starting from proper time $\tau_0 = 0.6$ fm/c after the collision [21]. We implement a small specific shear viscosity, $\eta/s = 0.047$ [22], and the 2+1 equation of state from lattice QCD [23]. Fluid elements hadronize [24] when reaching a temperature of 150 MeV. We include all hadronic resonances in the freezeout process (from the PDG16+ list [25]), and their subsequent strong decays, but we neglect rescattering in the hadronic phase [17, 26, 27].

Each hydrodynamic "event" corresponds to a different initial condition [28–31]. The output of hydrodynamics is the continuous probability distribution of the transverse momentum [32, 33], which one integrates to calculate the mean value, $\langle p_t \rangle$. Therefore, the statistical fluctuations mentioned in the discussion of Fig. 1, due to the finite event multiplicity, are absent in the hydrodynamic calculation, so that the event-to-event fluctuations of $\langle p_t \rangle$ are the dynamical fluctuations themselves. The histogram of the distribution of $\langle p_t \rangle$ is displayed as solid lines in Fig. 2 for two different centrality windows. Note that the values of $\langle p_t \rangle$ are larger than in Fig. 1, because the collision energy is much higher.[2] The width of the $\langle p_t \rangle$ distribution is comparable in Fig. 1 and in Fig. 2(a), in agreement with the evolution of dynamical $\langle p_t \rangle$ fluctuations from 200 GeV to 2.76 TeV collision energy observed in data [4]. Since the experimental distribution in Fig. 1

includes statistical fluctuations on top of the dynamical ones, one would expect it to be broader than our prediction, while this is not the case. In fact, our model of initial conditions overestimates the width of dynamical fluctuations by about a factor 2, which is a common discrepancy between hydrodynamic models and data [34, 35]. The distributions of $\langle p_t \rangle$ in Fig. 2 are clearly asymmetric, with a long tail on the right. This positive skew is more pronounced in peripheral collisions [panel (b)] than in central collisions [panel (a)].

A few remarks are in order. The qualitative prediction that the skewness is positive is to some extent trivial when fluctuations are large. The reason is that the transverse momentum is positive by construction, so that there is a strict lower bound on $\langle p_t \rangle$, but no upper bound. This naturally produces the left-right asymmetry seen in Fig. 2(b), in particular in small systems, where fluctuations are large (see e.g. Fig. 3 of Ref. [36] for an illustration).[3] Additionally, if one consider that a large system is given by the superimposition of statistically independent smaller clusters, then the positive skewness is carried over from the small systems to the larger one, because cumulants (to be defined in Sec. III) are additive.

We conclude that it is crucial to have quantitative measures of the skewness, and to assess how large its value should be in order for it to be considered non trivial.

III. MEASURING THE SKEWNESS

A quantitative measure of the skewness of a random variable x is the third centered moment, $\langle (x - \langle x \rangle)^3 \rangle$, where angular brackets denote an average value with respect to the probability distribution of x. It is usually positive when the tail is larger to the right than to the left, as in Figs. 1 and 2. The skewness is the third term in a systematic cumulant expansion, whose first and second terms are the mean and the variance, respectively.

A. Experimental analysis

We first recall how the mean value of the p_t distribution in a centrality class, which we denote by $\langle\langle p_t \rangle\rangle$, is evaluated in heavy-ion experiments. There are two ways of defining it, depending on whether one first averages over particles in an event [2], and then over all events, or whether one does both averages simultaneously [5].

―――――

[1] We use $p = 0$, corresponding to a geometric average of nuclear thickness functions. The thickness of a nucleus is a linear superimposition of participant nucleon thicknesses, which are taken as Gaussian profiles of width $w = 0.51$ fm. The normalization of each nucleon thickness fluctuates following a gamma distribution of unit mean and standard deviation $1/\sqrt{k}$, where we use $k = 1.6$.

[2] Also, our calculation overestimates $\langle p_t \rangle$ by a few percent even at the higher energy, as discussed in Ref. [12].

―――――

[3] Similarly, the upper bound on initial anisotropies, $\varepsilon_n < 1$, naturally generates non-Gaussian fluctuations that are crucial to understand experimental data in anisotropic flow fluctuations in peripheral nucleus-nucleus collisions [37–39] and in small systems [40, 41].
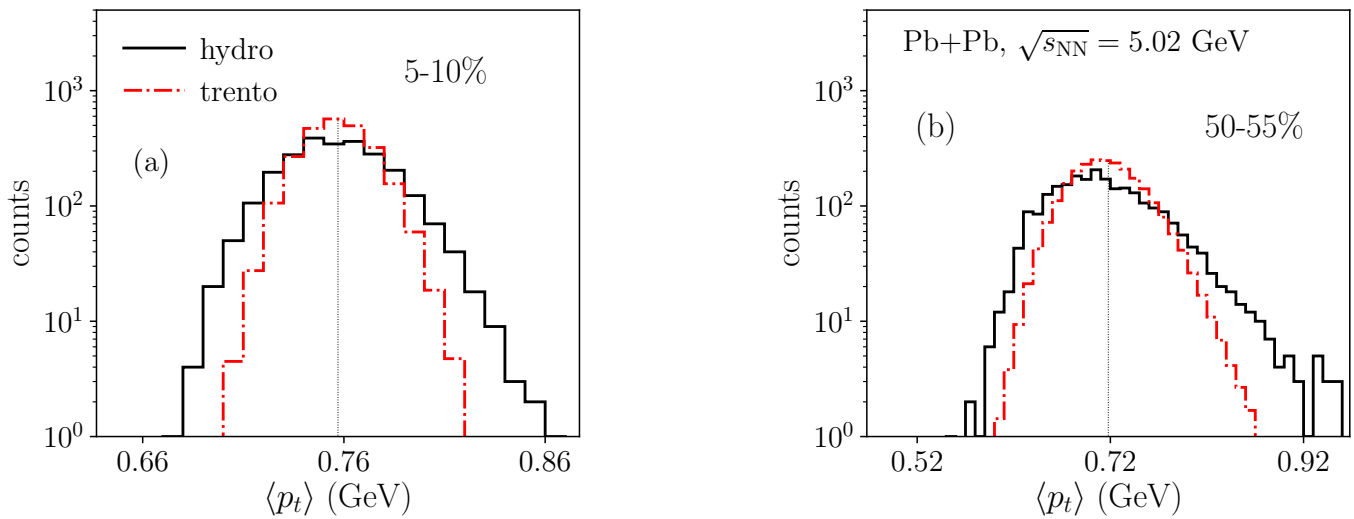
FIG. 2. (Color online) Solid lines: Distribution of $\langle p_t \rangle$ in event-by-event hydrodynamic simulations of Pb+Pb collisions at $\sqrt{s_{NN}} = 5.02$ TeV [12], for charged particles in the transverse momentum interval $0.2 < p_t < 3$ GeV and in the pseudorapidity interval $|\eta| < 0.8$. Dash-dotted line: Distribution of E_0/S, where E_0 and S are, respectively, the total energy and total entropy in the fluid at the beginning of the hydrodynamic evolution (see Sec. V). In order to facilitate the comparison, the value of E_0/S has been multiplied by a constant in each panel so that the mean matches that of the $\langle p_t \rangle$ distribution. (a) 5-10% centrality. (b) 50-55% centrality.

Specifically, the STAR collaboration defines [2]:

$$\langle\langle p_t \rangle\rangle_{\text{STAR}} \equiv \left\langle \frac{\sum_{i=1}^{N_{ch}} p_i}{N_{ch}} \right\rangle, \tag{1}$$

where N_{ch} denotes the number of charged particles in an event, p_i is the transverse momentum of the ith particle, and angular brackets denote an average over events in a centrality class. On the other hand, the ALICE collaboration defines [5]:

$$\langle\langle p_t \rangle\rangle_{\text{ALICE}} \equiv \frac{\left\langle \sum_{i=1}^{N_{ch}} p_i \right\rangle}{\langle N_{ch} \rangle}. \tag{2}$$

These definitions are almost equivalent, but not strictly equivalent when the multiplicity N_{ch} fluctuates event to event.

Either convention can be used when analyzing the variance of dynamical p_t fluctuations. We denote this variance by $\langle \Delta p_i \Delta p_j \rangle$, where the subscripts i, j are meant to

remind that it is constructed from pair correlations, with $i \neq j$. The STAR collaboration defines it as [2]:

$$\langle \Delta p_i \Delta p_j \rangle_{\text{STAR}} \equiv \left\langle \frac{\sum_{i,j \neq i} (p_i - \langle\langle p_t \rangle\rangle)(p_j - \langle\langle p_t \rangle\rangle)}{N_{ch}(N_{ch}-1)} \right\rangle, \tag{3}$$

where $\langle\langle p_t \rangle\rangle$ is defined by Eq. (1), while the ALICE collaboration defines it as [5]:

$$\langle \Delta p_i \Delta p_j \rangle_{\text{ALICE}} \equiv \frac{\left\langle \sum_{i,j \neq i} (p_i - \langle\langle p_t \rangle\rangle)(p_j - \langle\langle p_t \rangle\rangle) \right\rangle}{\langle N_{ch}(N_{ch}-1) \rangle}, \tag{4}$$

where $\langle\langle p_t \rangle\rangle$ is defined by Eq. (2). Note that even though Eqs. (3) and (4) involve double sums over i and j, they can be expressed in terms of simple sums, which are much faster to compute. The corresponding formulas for Eq. (3) are derived in Appendix A. The skewness is the third centered moment, which we denote by $\langle \Delta p_i \Delta p_j \Delta p_k \rangle$. It is defined by straightforward generalizations of Eqs. (3) and (4):

$$\langle \Delta p_i \Delta p_j \Delta p_k \rangle_{\text{STAR}} \equiv \left\langle \frac{\sum_{i,j \neq i, k \neq i,j} (p_i - \langle\langle p_t \rangle\rangle)(p_j - \langle\langle p_t \rangle\rangle)(p_k - \langle\langle p_t \rangle\rangle)}{N_{ch}(N_{ch}-1)(N_{ch}-2)} \right\rangle, \tag{5}$$

where $\langle\langle p_t \rangle\rangle$ is defined by Eq. (1), and

$$\langle \Delta p_i \Delta p_j \Delta p_k \rangle_{\text{ALICE}} \equiv \frac{\left\langle \sum_{i,j \neq i, k \neq i,j} (p_i - \langle\langle p_t \rangle\rangle)(p_j - \langle\langle p_t \rangle\rangle)(p_k - \langle\langle p_t \rangle\rangle) \right\rangle}{\langle N_{ch}(N_{ch}-1)(N_{ch}-2) \rangle}, \tag{6}$$

where $\langle\langle p_t \rangle\rangle$ is defined by Eq. (2). An efficient way of com-

puting Eq. (5) is detailed in Appendix A. Note that the

ATLAS collaboration follows the same convention as the STAR collaboration in its recent analysis of transverse momentum fluctuations [42].

B. Dimensionless observables

We now define two dimensionless measures of the skewness, which should have less sensitivity to analysis details, in particular the acceptance in p_t, which varies depending on the detector. The first measure is the standardized skewness, γ [37], here defined by:

$$\gamma_{p_t} \equiv \frac{\langle \Delta p_i \Delta p_j \Delta p_k \rangle}{\langle \Delta p_i \Delta p_j \rangle^{3/2}}. \tag{7}$$

While this is a dimensionless quantity, one expects it to depend on centrality and system size, as measured by the number of participant nucleons, N_{part}, for the following reasons. If one assumes that dynamical fluctuations scale with the multiplicity in the same way as statistical fluctuations[4], then the variance is approximately proportional to $1/N_{\mathrm{part}}$, and the skewness to $1/N_{\mathrm{part}}^2$ [44]. Hence, one expects the standardized skewness to be proportional to $1/\sqrt{N_{\mathrm{part}}}$.[5] Therefore, this quantity should be larger for peripheral collisions than for central collisions, which can be actually seen by eye in the comparison between Fig. 2(a) and Fig. 2(b). The fact that the standardized skewness decreases with N_{part} is in fact a consequence of the central limit theorem, which states that fluctuations are more Gaussian for a large system.

In order to eliminate this trivial size dependence, we introduce a second measure of the skewness, which we dub the *intensive* skewness, and denote by Γ:

$$\Gamma_{p_t} \equiv \frac{\langle \Delta p_i \Delta p_j \Delta p_k \rangle \langle\langle p_t \rangle\rangle}{\langle \Delta p_i \Delta p_j \rangle^2}. \tag{8}$$

With the above scaling rules, Γ_{p_t} is *independent* of N_{part}. This intensive measure of the skewness allows us address the comment raised at the end of Sec. II, that a positive skewness is to some extent trivial because $\langle p_t \rangle$ is itself positive. The typical trivial continuous distribution with positive support is the gamma distribution, which can be viewed as the equivalent of the Gaussian distribution for a random variable which is positive [45]. For the gamma distribution, the intensive skewness is a universal constant, $\Gamma = 2$.[6] This value is a useful baseline: An intensive skewness significantly larger than 2 should be considered nontrivial.

---

[4] This is approximately true in the Glauber Monte Carlo model [43], where dynamical fluctuations originate from the positions of participant nucleons, and the multiplicity, responsible for the statistical fluctuations, it itself roughly proportional to N_{part}.

[5] These scaling rules are verified in a toy model in Appendix B.

[6] Similarly, one obtains $\Gamma = 1$ for the discrete Poisson distribution.
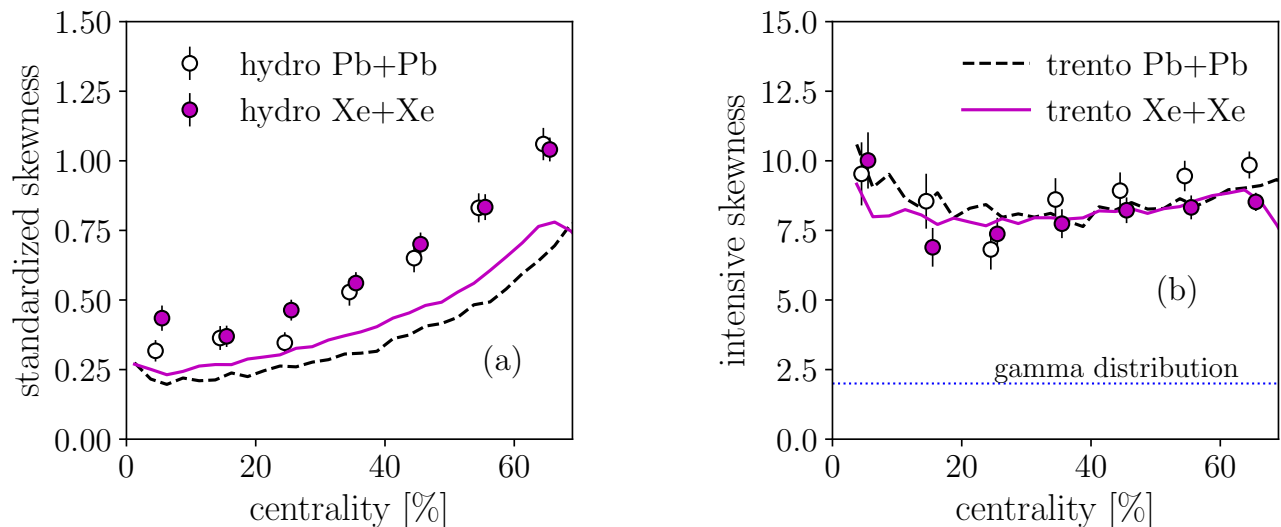
IV. HYDRODYNAMIC PREDICTIONS

Evaluating the skewness in event-by-event hydrodynamics is much simpler than in experiment. As explained above, one evaluates $\langle p_t \rangle$ for each initial condition by integrating the continuous momentum distribution resulting from the hydrodynamic expansion. The mean transverse momentum in a centrality class, $\langle\langle p_t \rangle\rangle$, is obtained by averaging $\langle p_t \rangle$ over initial conditions. The variance and the skewness are then defined by:

$$\langle \Delta p_i \Delta p_j \rangle_{\mathrm{hydro}} = \left\langle \left(\langle p_t \rangle - \langle\langle p_t \rangle\rangle \right)^2 \right\rangle$$
$$\langle \Delta p_i \Delta p_j \Delta p_k \rangle_{\mathrm{hydro}} = \left\langle \left(\langle p_t \rangle - \langle\langle p_t \rangle\rangle \right)^3 \right\rangle, \tag{9}$$

where the outer angular brackets denote an average over initial conditions.

Figure 3 presents our prediction for the standardized skewness [panel (a)], and the intensive skewness [panel (b)] for Xe+Xe and Pb+Pb collisions, as a function of the centrality percentile, using the same hydrodynamic calculation as in Sec. II.

The standardized skewness in panel (a) increases as a function of the centrality percentile, as already observed in Fig. 2, reflecting the fact that larger centrality implies a smaller number of participant nucleons. One also expects the standardized skewness to be larger in the smaller system, Xe+Xe, although, within our numerical precision, this is not observed in all the centrality bins. It is interesting to compare γ_{p_t} to the standardized skewness of elliptic flow fluctuations in the reaction plane, say γ_{v_2}, measured in Refs. [38, 39]. One notes in particular that γ_{p_t} is in magnitude twice as large as γ_{v_2}, even in peripheral collisions, where the distribution of v_2 originates from a distribution of initial eccentricity, ε_2, which is strongly skewed due to the upper bound $\varepsilon_2 < 1$ [37].

The intensive skewness in panel (b) is instead approximately independent of both the collision species and the collision centrality. It is in the range $7 < \Gamma_{p_t} < 10$, much larger than the baseline $\Gamma_{p_t} = 2$ for a gamma distribution. The predictive value of our hydrodynamic calculation is limited by the fact that it overestimates the variance of $\langle p_t \rangle$ fluctuations, as mentioned in Sec. II. A broader distribution is typically more skewed, therefore, we expect that our calculation will overestimate future experimental data on the standardized skewness. We expect on the other hand that much of this error cancels in the intensive skewness, which should represent a more solid prediction. Thus, we expect the intensive skewness, Γ_{p_t}, in 5.02 TeV Pb+Pb collisions to lie between 7 and 10. We stress that this value implies a nontrivial distribution of $\langle p_t \rangle$.

V. ORIGIN OF THE SKEWNESS

We now investigate the origin of the large positive skewness of $\langle p_t \rangle$ fluctuations found in hydrodynamic calculations. As it was shown in Refs. [8, 9], if one looks at

FIG. 3. (Color online) Hydrodynamic predictions for: (a) the standardized skewness, γ_{p_t}, defined by Eq. (7); (b) the intensive skewness, Γ_{p_t}, defined by Eq. (8), in Pb+Pb collisions at $\sqrt{s_{NN}} = 5.02$ TeV (open symbols) and Xe-Xe collisions at $\sqrt{s_{NN}} = 5.44$ TeV (full symbols), as a function of the centrality percentile. Error bars represent the statistical error, due to the finite number of hydrodynamic events, estimated via jackknife resampling. The open and full symbols have been slightly shifted to the left and to the right, respectively, for the sake of readability. Lines are the same quantities as symbols, where one replaces $\langle p_t \rangle$ with the value of E_0/S at the beginning of the hydrodynamic evolution (Sec. V). The dotted line in panel (b) represents the expected baseline for the intensive skewness, i.e., the intensive skewness of a gamma distribution.

events with the same *initial* entropy (which experimentally can be achieved to a good approximation by fixing the final-state multiplicity), then $\langle p_t \rangle$ is tightly correlated with the total energy of the fluid at the beginning of the hydrodynamic evolution, E_0. Intuitively, this is due to the fact that the momentum is a function of the energy, and thus, if the number of particles is fixed, it is the energy that determines the mean transverse momentum. The nontrivial aspect of this correspondence is that the correlation of $\langle p_t \rangle$ is tighter with the initial energy, E_0, than with the energy at freeze-out [8], even though particles are emitted at freeze-out. The goal of this section is to show that, at fixed centrality, one expects the skewness of $\langle p_t \rangle$ fluctuations to be driven by the skewness of E_0 fluctuations.

Although the relation between $\langle p_t \rangle$ and E_0 is not quite linear, we can relate their fluctuations in a simplified, *effective* hydrodynamic description [46]. This description replaces the space-time evolution of the quark-gluon plasma with an equivalent uniform gas at an effective temperature, T, that contains the same total entropy and total energy as the quark-gluon plasma at freezeout. In this effective description, the final-state $\langle p_t \rangle$ is proportional to T, whereas E_0 is proportional to ϵ/s, where the energy density, ϵ, and the entropy density, s, are evaluated at temperature T. The fluctuations of E_0 and those of $\langle p_t \rangle$ can be then related through the equation of state.

Let us first derive a relation between the relative variation of $\langle p_t \rangle$ and that of E_0 in the regime of small fluctuations. First note that the relative $\langle p_t \rangle$ variation is related

to that of the entropy density, s, through:

$$d\ln\langle p_t \rangle = d\ln T = c_s^2 d\ln s, \tag{10}$$

where $c_s = (d\ln T/d\ln s)^{1/2}$ is the speed of sound at temperature T. Similarly, the relative variation of E_0 is given by:

$$\begin{aligned} d\ln E_0 = d\ln\left(\frac{\epsilon}{s}\right) &= \frac{d\epsilon}{\epsilon} - \frac{ds}{s} \\ &= \frac{Tds}{\epsilon} - \frac{ds}{s} = \frac{(\epsilon+P)ds - \epsilon ds}{\epsilon s} \\ &= (P/\epsilon)d\ln s, \end{aligned} \tag{11}$$

where we have used the thermodynamic identities $d\epsilon = Tds$ and $\epsilon + P = Ts$. Combining the last two equations, one predicts

$$\frac{\sigma(\langle p_t \rangle)}{\langle\langle p_t \rangle\rangle} = c_s^2 \frac{\epsilon}{P} \frac{\sigma(E_0)}{\langle E_0 \rangle} \simeq 1.24 \frac{\sigma(E_0)}{\langle E_0 \rangle} \tag{12}$$

where $\sigma(\langle p_t \rangle)$ and $\sigma(E_0)$ denote, respectively, the standard deviation of $\langle p_t \rangle$ and E_0, and, in the last equality, we have used $T = 222$ MeV for 5.02 TeV Pb+Pb collisions [46], at which we have evaluated the thermodynamic quantities using the lattice QCD equation of state [23]. Note that the relative fluctuations of E_0 is equal to that of E_0/S, where S is the total entropy, when S is kept fixed. To correct for potential effects of finite-sized centrality intervals, or entropy production due to viscosity, one should replace E_0 by E_0/S in Eq. (12). To prove that the latter equation provides a meaningful prediction, we show in Fig. 2 the distribution of E_0/S,

multiplied by an appropriate factor so that it presents the same mean value as the $\langle p_t \rangle$ distribution. One sees by eye that the distribution of $\langle p_t \rangle$ is broader than that of E_0/S in relative value, more precisely, by a factor 1.3 in panel (a) and by a factor 1.6 in panel (b). Equation (12) thus correctly predicts that the fluctuations of $\langle p_t \rangle$ are larger than those of E_0/S, albeit not quantitatively.

Let us move then to the skewness. An analogous derivation of the standardized skewness, γ, and of the intensive skewness, Γ, in the effective framework yields $\gamma_{p_t} \simeq \gamma_{E_0}$, and $\Gamma_{p_t} \simeq 0.8\Gamma_{E_0}$. These relations imply that the skewness of $\langle p_t \rangle$ fluctuations is indeed expected to be driven by that of E_0 fluctuations. Figure 3 displays the standardized skewness and the intensive skewness of the distribution of E_0/S, which in practice is obtained by replacing $\langle p_t \rangle$ with E_0/S in the right-hand side of Eq. (9). We note that the standardized skewness [Fig. 3(a)] of E_0/S fluctuations is indeed positive, and of order 0.25 in central collisions. In more peripheral collisions it is somewhat smaller than the skewness of $\langle p_t \rangle$ fluctuations. Note that γ_{E_0} is larger in Xe+Xe collisions than in Pb+Pb collisions, as expected from the smaller system size. Moving to the intensive skewness in Fig. 3(b), it is almost identical for E_0/S and for $\langle p_t \rangle$, which implies that the distribution of E_0 in the T$_R$ENTo model is nontrivial. As expected, the intensive skewness of E_0 is essentially independent of system size, i.e., of the centrality.

On the whole, the predictions of the effective framework are qualitatively correct, and we conclude that the main features displayed by the skewness of $\langle p_t \rangle$ fluctuations stem from the skewness of the initial energy, E_0. Note that a more quantitative understanding may be achieved by improving the initial-state predictor. In a recent preprint Schenke, Shen and Teaney [47] studied the goodness of various estimators of $\langle p_t \rangle$, and found that an improved predictor, especially for peripheral collisions, can be obtained by adding a dependence on the elliptical area of the system [6]. We do not investigate this possibility here.

VI. RELATING THE SKEWNESS TO INITIAL DENSITY FLUCTUATIONS

The results of the previous section show that the skewness of $\langle p_t \rangle$ fluctuations originates from the skewness of E_0 fluctuations. The fact that the latter skewness is positive, though, is specific to the model used in the numerical evaluation, i.e., a T$_R$ENTo parametrization tuned to reproduce some sets of experimental data. In this section, we argue that the prediction that $\langle p_t \rangle$ fluctuations have positive skewness is more general, and does not rely on a specific model of initial conditions. For this purpose, we derive formulas for the variance and the skewness of E_0 fluctuations for a generic fluctuating initial density profile.

A. Formalism

Our study is limited to boost-invariant ideal hydrodynamics for simplicity, and neglects initial transverse flow [18, 20]. The hydrodynamic evolution is then determined by the entropy density field at the initial condition, $s(x)$, where x denotes a point in the transverse plane. We consider an ensemble of events with the same geometry (same positions of incoming nuclei) and same total entropy, $\int s(x)dx$. The fluctuations of the field $s(x)$ within this ensemble of events can be characterized by its n-point correlation functions. We assume that, for any event, $s(x)$ can be decomposed as a fluctuation on top of a background: $s(x) = \langle s(x) \rangle + \delta s(x)$, where $\langle s(x) \rangle$, or 1-point function, is the average value of $s(x)$ for a fixed x, and $\delta s(x)$ is the fluctuation. Observables are evaluated through a perturbative expansion in powers of the fluctuation. This approach is identical to that of Refs. [10, 36, 44, 48], the only difference being that we take now $s(x)$ as the fundamental field instead of the energy density, $\epsilon(x)$.

The condition that the total entropy is fixed implies:

$$\int_x \delta s(x) = 0, \tag{13}$$

where we use the shortcut $\int_x$ for the integration over the transverse plane, which is a double integral. The connected 2-point function is the average over events of $\delta s(x_1)\delta s(x_2)$. It characterizes how fluctuations at different points x_1 and x_2 are correlated with one another. We assume that all fluctuations are local, which implies that correlations are short ranged. Under this condition, one can write the two-point function in the form [36]:

$$\langle \delta s(x_1)\delta s(x_2) \rangle = \kappa_2(x_1)\delta(x_1 - x_2) - \frac{\kappa_2(x_1)\kappa_2(x_2)}{\int_x \kappa_2(x)}, \tag{14}$$

where we assimilate the short range correlation to a Dirac peak, $\delta(x_1 - x_2)$, with a positive x-dependent amplitude, $\kappa_2(x)$, which represents the density of variance of the entropy field. Equation (13) implies that the two-point function must vanish upon integration over x_1 or x_2. This is guaranteed by the last term in the right-hand side of Eq. (14).

To evaluate the skewness, we shall also need the three-point function of the density field. As shown in Ref. [36], for short-range correlations the three-point function at fixed total entropy can be written in the form:

$$\langle \delta s(x_1)\delta s(x_2)\delta s(x_3) \rangle = \kappa_3(x_1)\delta(x_1 - x_2)\delta(x_1 - x_3)$$
$$- \frac{\kappa_3(x_1)\delta(x_1 - x_2)\kappa_2(x_3) + \text{perm.}}{\int_x \kappa_2(x)}$$
$$+ \frac{\kappa_3(x_1)\kappa_2(x_2)\kappa_2(x_3) + \text{perm.}}{\left(\int_x \kappa_2(x)\right)^2}$$
$$- \frac{\int_x \kappa_3}{\left(\int_x \kappa_2\right)^3}\kappa_2(x_1)\kappa_2(x_2)\kappa_2(x_3),$$
$$\tag{15}$$

where the second and third lines must be summed over circular permutations of x_1, x_2, x_3. The first term in the right-hand side is the contribution of the short-range correlation, and $\kappa_3(x)$ is the "density of skewness", in the same way as $\kappa_2(x)$ is the density of variance. Note that $\kappa_3(x)$ is typically positive everywhere (e.g. for Poisson fluctuations), even though this is not a mathematical requirement. The additional terms in Eq. (15) are contributions from the condition that all events have the same total entropy. This expression is consistent with the sum rule (13), as can be checked upon integration over x_1 (or x_2 or x_3, by symmetry). Note that the three-point function involves both $\kappa_2(x)$ and $\kappa_3(x)$, and it is linear in $\kappa_3(x)$.

B. Variance of initial energy fluctuations

Equipped with this formalism, we evaluate the fluctuations of the initial energy, E_0. This quantity is given by the integral of the energy density, $\epsilon(x)$, which is related to $s(x)$ through the equation of state:

$$E_0 = \int_x \epsilon\left(s(x)\right). \tag{16}$$

We then write $s(x) = \langle s(x) \rangle + \delta s(x)$, and expand in powers of $\delta s(x)$. To first order in $\delta s(x)$, one can write $E_0 = \langle E_0 \rangle + \delta E_0$, with

$$\langle E_0 \rangle = \int_x \epsilon(\langle s(x) \rangle),$$
$$\delta E_0 = \int_x T(x)\delta s(x), \tag{17}$$

where $T(x)$ is the temperature corresponding to the average entropy density, $\langle s(x) \rangle$, and we have used the thermodynamic identity $d\epsilon = Tds$. The variance of the energy is:

$$\langle \delta E_0^2 \rangle = \int_{x_1,x_2} T(x_1)T(x_2)\langle \delta s(x_1)\delta s(x_2) \rangle. \tag{18}$$

Using the expression (14) of the two-point function, one obtains

$$\langle \delta E_0^2 \rangle = \int_x T(x)^2 \kappa_2(x) - \frac{\left(\int_x T(x)\kappa_2(x)\right)^2}{\int_x \kappa_2(x)}, \tag{19}$$

where the last term in the right-hand side comes from the condition that the total entropy is fixed. We define an average temperature, $\bar{T}$, by:

$$\bar{T} \equiv \frac{\int_x T(x)\kappa_2(x)}{\int_x \kappa_2(x)}. \tag{20}$$

With this notation, Eq. (19) can be rewritten as

$$\langle \delta E_0^2 \rangle = \int_x (T(x) - \bar{T})^2 \kappa_2(x). \tag{21}$$

Note that the condition that all events have the same total entropy results in the substitution $T(x) \to T(x) - \bar{T}$.

Let us comment on the physical implication of Eq. (21). In this equation, $T(x)$ denotes the temperature profile at the beginning of the hydrodynamic expansion, that is, when the temperature is the highest, and $\bar{T}$ its value averaged over x. The difference $T(x) - \bar{T}$ is a temperature difference, which is proportional to c_s^2. Therefore, one expects the relative fluctuation of E_0 to be itself proportional to c_s^2, where c_s is the velocity of sound at the beginning of the hydrodynamic calculation. This is checked by an explicit calculation in Appendix B 2. This correspondence only holds in ideal hydrodynamics, and viscous corrections are large at early times, therefore, its relevance to the phenomenology is questionable. However, it suggests that the physics of $\langle p_t \rangle$ fluctuations might open a window onto early-time thermodynamics.

C. Skewness of initial energy fluctuations

We now evaluate the skewness of the distribution of E_0. This is a higher-order quantity, therefore, we need to expand the energy density to order 2 in δs:

$$\epsilon(s(x)) = \epsilon(\langle s(x) \rangle) + T(x)\delta s(x) + \frac{1}{2}T'(x)\delta s(x)^2, \tag{22}$$

where we define

$$T'(x) \equiv \frac{dT}{ds} = c_s^2(x)\frac{T(x)}{\langle s(x) \rangle}, \tag{23}$$

where $c_s(x)$ is the speed of sound at the temperature $T(x)$. With the second order term taken into account, Eq. (17) is replaced by:

$$\langle E_0 \rangle = \int_x \epsilon(\langle s(x) \rangle) + \frac{1}{2}\int_x T'(x)\langle \delta s(x)^2 \rangle,$$
$$\delta E_0 = \int_x T(x)\delta s(x) + \frac{1}{2}\int_x T'(x)\left(\delta s(x)^2 - \langle \delta s(x)^2 \rangle\right). \tag{24}$$

The skewness is the third centered moment, that is, $\langle \delta E_0^3 \rangle$. To leading order in the fluctuations, one must keep all terms of order 3 and 4 in δs, which contribute to the same order after averaging over events. We write

$$\langle \delta E_0^3 \rangle = \langle \delta E_0^3 \rangle_3 + \langle \delta E_0^3 \rangle_4, \tag{25}$$

where we separate the contributions of terms of order δs^3 and δs^4.

The contribution of order δs^3 is obtained by keeping only the first term in the second line of Eq. (24):

$$\langle \delta E_0^3 \rangle_3 = \int_{x_1,x_2,x_3} T(x_1)T(x_2)T(x_3)\langle \delta s(x_1)\delta s(x_2)\delta s(x_3) \rangle. \tag{26}$$

It involves the three-point function of the density field. Inserting Eq. (15) into Eq. (26), one obtains, after some algebra, a compact result:

$$\langle \delta E_0^3 \rangle_3 = \int_x \left(T(x) - \bar{T} \right)^3 \kappa_3(x), \qquad (27)$$

where $\bar{T}$ is defined by Eq. (20). As in Eq. (21), the condition that all events have the same entropy results in the substitution $T(x) \to T(x) - \bar{T}$.

We finally evaluate $\langle \delta E^3 \rangle_4$, which is the contribution obtained by expanding two factors of δE to order δs and the third factor to order δs^2. One is led to evaluate the average value of quantities such as:

$$A(x_1, x_2, x_3) \equiv \delta s(x_1) \delta s(x_2) \left(\delta s(x_3)^2 - \langle \delta s(x_3)^2 \rangle \right), \qquad (28)$$

where four-point averages can be computed using Wick's theorem, which gives:

$$\langle A(x_1, x_2, x_3) \rangle = 2 \langle \delta s(x_1) \delta s(x_3) \rangle \langle \delta s(x_2) \delta s(x_3) \rangle, \quad (29)$$

where the right-hand side involves the 2-point function, Eq. (14). After some algebra, one obtains

$$\langle \delta E_0^3 \rangle_4 = 3 \int_x (T(x) - \bar{T})^2 T'(x) \kappa_2(x)^2. \qquad (30)$$

The integrand is everywhere positive, so that $\langle \delta E_0^3 \rangle_4$ is positive. It is interesting to note that the intermediate calculations involve the variance of the entropy density at a given point, i.e., the term $\langle \delta s(x)^2 \rangle$ in Eq. (24). This quantity is sensitive to the scale of inhomogeneities [15], that is, to the transverse size of the "hot spots" in the initial density profile. However, this dependence cancels in Eq. (29), and the final results depend only on the functions $\kappa_n(x)$, which are integrated over the relative distance. This implies that both the width of $\langle p_t \rangle$ fluctuations and their skewness should have limited sensitivity to short-range, subnucleonic fluctuations, in the same way as anisotropic flow fluctuations [15, 49–51]. They are on the other hand potentially useful probes of early-time thermodynamics, as suggested at the end of Sec. VI B.

To conclude, let us write down our final formula for the skewness, Eq. (25). It is the sum of the contributions (27) and (30):

$$\langle \delta E_0^3 \rangle = \int_x \left(T(x) - \bar{T} \right)^3 \kappa_3(x) + 3 \int_x (T(x) - \bar{T})^2 T'(x) \kappa_2(x)^2. \qquad (31)$$

The second term is always positive, while the first contribution is typically negative, but smaller in magnitude. In Appendix B we check explicitly that, in the simple case of identical, localized sources with a Gaussian distribution, where all integrals can be carried out analytically, the second term indeed dominates over the first term so that the skewness is positive. The contribution (30) provides, thus, a model-independent explanation for the positive skewness of E_0 fluctuations, and consequently of $\langle p_t \rangle$ fluctuations.

VII. CONCLUSIONS

Hydrodynamics predicts that the event-by-event fluctuations of the mean transverse momentum, $\langle p_t \rangle$, have positive skew. This prediction could be verified straightforwardly in experiments, following the analysis procedures explained in this manuscript. Along with the standardized skewness, we have introduced a new dimensionless measure, the intensive skewness, which, on the basis of hydrodynamic calculations, should lie between 7 and 10 in nucleus-nucleus collisions, and be approximately independent of the collision centrality and of the size of the colliding nuclei. We have shown that these predictions are generic, and can be traced back to the fact that $\langle p_t \rangle$ fluctuations result from fluctuations of the energy of the fluid when the hydrodynamic expansion starts. This confirms in particular that dynamical $\langle p_t \rangle$ fluctuations are a collective effect, much in the same way as anisotropic flow. It also implies, more specifically, that they are sensitive to the early temperature. The average transverse momentum itself has proven able to give insight about the thermodynamics of the quark-gluon plasma, at a temperature around $T \sim 220$ MeV in 5.02 TeV Pb-Pb collisions [46]. Our preliminary study suggests that, on the other hand, higher-order cumulants, such as the skewness, might serve as detailed probes of QCD thermodynamics at higher temperatures, achieved during the early stages of the collision.

Appendix A: Coding the skewness analysis

In this Appendix, we explain how to efficiently compute the skewness. We choose the first definition, Eq. (5), but similar algebraic manipulations can be carried out to simplify the second definition, Eq. (6). In every event, one evaluates the moments of the p_t distributions, defined by

$$Q_n = \sum_{i=1}^{N_{\rm ch}} (p_i)^n, \qquad (A1)$$

where $n = 1, 2, 3$, p_i is the transverse momentum of particle i, and the sum runs over all the charged particles detected in the event. Sums over pairs and triplets of

particles can be expressed simply in terms of these moments:

$$\sum_{i,j\neq i} p_i p_j = (Q_1)^2 - Q_2,$$

$$\sum_{i,j\neq i, k\neq i,j} p_i p_j p_k = (Q_1)^3 - 3Q_2 Q_1 + 2Q_3. \qquad \text{(A2)}$$

These equations express the multiple sums in the left-hand side in terms of simple sums, which are faster to evaluate. They are specific cases of Eqs. (11) and (14) of Ref. [52] in the case of a unique set of particles, $A_1 = A_2 = A_3$.

With these notations, Eqs. (1) and (3) can be rewritten

in the form:

$$\langle\langle p_t \rangle\rangle_{\text{STAR}} = \left\langle \frac{Q_1}{N_{\text{ch}}} \right\rangle,$$

$$\langle \Delta p_i \Delta p_j \rangle_{\text{STAR}} = \left\langle \frac{(Q_1)^2 - Q_2}{N_{\text{ch}}(N_{\text{ch}} - 1)} \right\rangle - \left\langle \frac{Q_1}{N_{\text{ch}}} \right\rangle^2,$$

(A3)

where angular brackets denote an average value over events in a narrow centrality bin. Note that these expressions are strictly equivalent to those used by the STAR collaboration (Eqs. (1)-(4) of Ref. [2]), even though they are written in a different form.

Finally, Eq. (5) can be rewritten in the form:

$$\langle \Delta p_i \Delta p_j \Delta p_k \rangle_{\text{STAR}} = \left\langle \frac{(Q_1)^3 - 3Q_2 Q_1 + 2Q_3}{N_{\text{ch}}(N_{\text{ch}} - 1)(N_{\text{ch}} - 2)} \right\rangle - 3 \left\langle \frac{(Q_1)^2 - Q_2}{N_{\text{ch}}(N_{\text{ch}} - 1)} \right\rangle \left\langle \frac{Q_1}{N_{\text{ch}}} \right\rangle + 2 \left\langle \frac{Q_1}{N_{\text{ch}}} \right\rangle^3.$$

This equation expresses the skewness in terms of the simple sums in Eq. (A1), which are much faster to compute than the multiple sums in Eq. (5). It has been advocated [47] that the analysis of $\langle p_t \rangle$ fluctuations should be done by enforcing rapidity gaps between the particles i, j, k, in the same way as analyses of anisotropic flow [53], in order to suppress correlations due to decay kinematics and other "nonflow" effects. The skewness is likely to be less affected by nonflow effects than the variance as it is a higher-order cumulant [54], but rapidity gaps can be easily implemented [52].

Appendix B: Simple model of density fluctuations

In this appendix, we present an explicit application of the perturbative approach of Sec. VI by working out a simple example, and we assess its validity by showing the comparison between perturbative results and exact results coming from a Monte Carlo calculation.

1. Identical sources

We model the entropy density at the beginning of the hydrodynamic evolution as the sum of N identical contributions [49], in the spirit of the Glauber modeling [43]:

$$s(x) = \sum_{i=1}^{N} \Delta(x - r_i), \qquad \text{(B1)}$$

where r_i are the positions of "sources", whose positions in the transverse plane are independent random variables with a probability distribution $p(r_i)$, and $\Delta(x)$ is a narrow peak centered around the origin. The total entropy is

$\int_x s(x) = N \int_x \Delta(x)$. Therefore, fixing the total entropy amounts to fixing the number of sources, N.

The n-point functions of this model can be evaluated explicitly in terms of N, $p(x)$ and $\Delta(x)$ [55]. The 1-point function is:

$$\langle s(x) \rangle = N \int_r p(r)\Delta(x - r), \qquad \text{(B2)}$$

while the 2-point function is:

$$\langle \delta s(x_1) \delta s(x_2) \rangle = N \int_r p(r)\Delta(x_1 - r)\Delta(x_2 - r)$$
$$- N \int_r p(r)\Delta(x_1 - r) \int_{r'} p(r')\Delta(x_2 - r').$$

(B3)

If the width of the function $\Delta(r)$ is much smaller than the scale over which $p(x)$ varies, one can neglect the variation of $p(x)$ across the extension of the source, and these equations simplify to:

$$\langle s(x) \rangle = N p(x) \int_r \Delta(r), \qquad \text{(B4)}$$

and

$$\langle \delta s(x_1) \delta s(x_2) \rangle = N p(x_1) \int_r \Delta(x_1 - r)\Delta(x_2 - r)$$
$$- N p(x_1)p(x_2) \left(\int_r \Delta(r) \right)^2. \qquad \text{(B5)}$$

Note that the latter equation is a specific case of Eq. (14), with

$$\kappa_2(x) = N p(x) \left(\int_r \Delta(r) \right)^2, \qquad \text{(B6)}$$

which amounts to assimilating the sources to Dirac delta peaks. A similar calculation [36] shows that the 3-point function has the same form as in Eq. (15), with

$$\kappa_3(x) = N p(x) \left(\int_r \Delta(r) \right)^3.$$ (B7)

Note that both $\kappa_2(x)$ and $\kappa_3(x)$ depend on the integral of $\Delta(x)$ over the plane and, thus, are independent of the actual shape of this function. This confirms somewhat more explicitly the previous argument that the variance and the skewness are indeed not sensitive to short-scale structures.

2. Gaussian density profile, constant c_s

To move forward, we need to specify the functional form of $p(r_i)$ and an equation of state. To obtain compact analytic expressions, we consider for simplicity that the distribution of sources in the transverse plane is Gaussian:

$$p(x) = \frac{1}{\pi\sigma^2} \exp\left(-\frac{x^2}{\sigma^2}\right).$$ (B8)

Then, according to Eq. (B4), the average entropy density profile is also Gaussian form. The energy density requires the knowledge of the equation of state. For simplicity, we consider a power-law equation of state:

$$T = s^{c_s^2},$$
$$\epsilon = \frac{s^{1+c_s^2}}{1+c_s^2},$$ (B9)

where c_s^2 is the velocity of sound. At early times (or high temperatures), $c_s^2 \simeq \frac{1}{3}$ in ideal hydrodynamic calculations using the lattice QCD equation of state.

We can thus proceed to the evaluation of the average temperature $\bar{T}$. If we denote by T_0 the temperature in the center, the average entropy density and the corresponding temperature profiles are given by:

$$\langle s(x) \rangle = T_0^{1/c_s^2} \exp\left(-\frac{x^2}{\sigma^2}\right),$$
$$T(x) = T_0 \exp\left(-\frac{c_s^2 x^2}{\sigma^2}\right).$$ (B10)

Identifying the first of these equations with Eq. (B4), one obtains:

$$\int_r \Delta(r) = \frac{\pi\sigma^2 T_0^{1/c_s^2}}{N}.$$ (B11)

This expression can be used to express $\kappa_2(x)$ and $\kappa_3(x)$, defined by Eqs. (B6) and (B7), as a function of N, c_s and T_0. Equation (20) then gives:

$$\bar{T} = \frac{T_0}{1 + c_s^2}.$$ (B12)

Finally, we can evaluate the mean, the variance, and the skewness of the initial energy, E_0, analytically using Eqs. (17), (21), (27), and (30). One obtains:

$$\langle E_0 \rangle = \frac{\pi\sigma^2}{(1+c_s^2)^2} T_0^{1+c_s^{-2}},$$

$$\langle \delta E_0^2 \rangle = \frac{1}{N} \frac{\left(c_s^2(1+c_s^2)\right)^2}{(1+2c_s^2)} \langle E_0 \rangle^2,$$

$$\langle \delta E_0^3 \rangle_3 = -\frac{1}{N^2}(2-2c_s^2) \frac{\left(c_s^2(1+c_s^2)\right)^3}{(1+5c_s^2+6c_s^4)} \langle E_0 \rangle^3,$$

$$\langle \delta E_0^3 \rangle_4 = \frac{1}{N^2}(3+3c_s^2+6c_s^4) \frac{\left(c_s^2(1+c_s^2)\right)^3}{(1+5c_s^2+6c_s^4)} \langle E_0 \rangle^3.$$ (B13)

The variance and the skewness are proportional to $1/N$ and $1/N^2$, respectively, as anticipated from the discussion in Sec. III B. The two contributions to the skewness in Eq. (25) are of the same order of magnitude. The first is negative while the second is positive, and larger in magnitude for any value of c_s^2. Note that, for a typical speed of sound, $c_s^2 = 1/3$, we find that $\langle \delta E_0^3 \rangle_4$ is larger than $\langle \delta E_0^3 \rangle_3$ by a factor 3. The positive term thus *dominates*. This is a clear indication that the positive skewness of E_0 fluctuations is generic, and that one can safely expect to observe it in any model of the initial state.

Finally, the relative standard deviation, the standardized skewness, and the intensive skewness are given, respectively, by:

$$\frac{\sqrt{\langle \delta E_0^2 \rangle}}{\langle E_0 \rangle} = \frac{1}{\sqrt{N}} \frac{c_s^2(1+c_s^2)}{\sqrt{1+2c_s^2}},$$

$$\gamma_{E_0} = \frac{1}{\sqrt{N}} \left(1+2c_s^2\right)^{3/2},$$

$$\Gamma_{E_0} = \frac{(1+2c_s^2)^2}{c_s^2(1+c_s^2)}.$$ (B14)

A few comments are in order. As anticipated in the discussion at the end of Sec. VI B, the relative fluctuation of E_0 is roughly proportional to c_s^2. The intensive skewness is independent of N, and inversely proportional to c_s^2. For $c_s^2 = \frac{1}{3}$, its value is 6.25, which is actually close to the intensive skewness of the more sophisticated T_RENTo calculation presented in Fig. 3(b).

3. Monte Carlo calculations

We check now the validity of the perturbative results by carrying out Monte Carlo simulations. To reproduce the model outlined in the previous section, the only additional ingredient to specify is the shape of a single source, $\Delta(x)$, appearing in Eq. (B1). One can use any function whose integral over the transverse plane is finite, since the final results do not depend on this choice, as argued
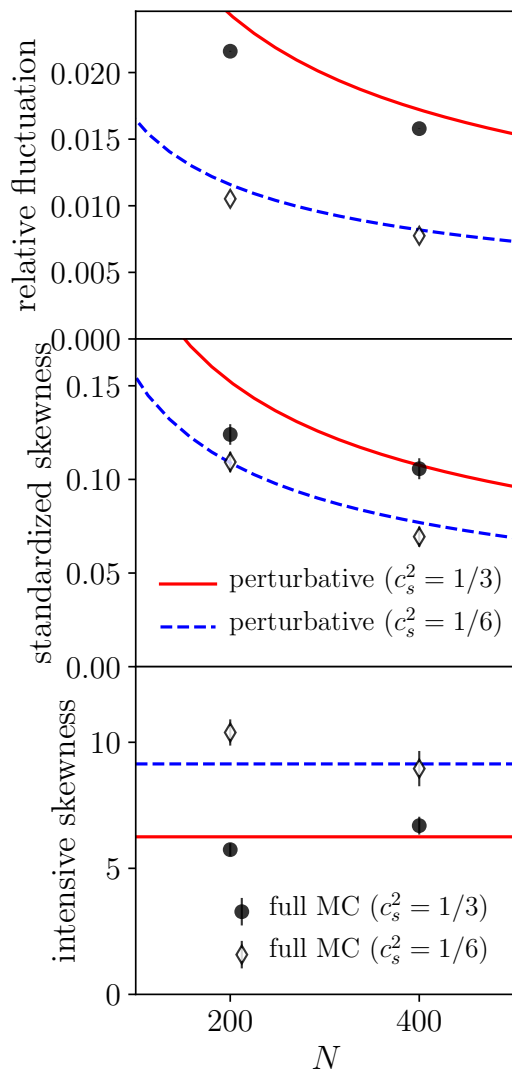
FIG. 4. (Color online) Symbols: Results of Monte Carlo (MC) simulations (see text). Lines: leading order perturbative expression given by Eq, (B14). Panels (a), (b) and (c) display the quantities corresponding to the three lines of these equations, respectively: relative standard deviation, standardized skewness, intensive skewness. The speed of sound is $c_s = 1/\sqrt{3}$ for the closed symbols and solid lines, while $c_s = 1/\sqrt{6}$ for the open symbols and dashed lines.

previously. For simplicity, we choose a Gaussian:

$$\Delta(x) \propto \exp\left(-\frac{x^2}{w^2}\right). \qquad (B15)$$

The validity of the perturbative calculation relies on two conditions. First, the width of $\Delta(x)$, w, must be small compared to the typical transverse extent of one event (as determined by the positions of N sources), which is in turn proportional to σ in Eq. (B8). Second, the standard deviation of the entropy density at a given point, obtained as the square root of Eq. (B5) after setting $x_2 = x_1$, must be smaller than the average density (B4) at the same point, in order for the Taylor expansion in Eq. (22) to be valid. Since in this source model the fluctuation of local quantities are determined by the density of sources at a given point, this is naturally a condition on the value of N. In formulas, the conditions we need to fulfill are:

$$\frac{w}{\sigma} \ll 1,$$
$$\frac{\sigma}{w\sqrt{N}} \ll 1. \qquad (B16)$$

We simply define w by:

$$w = N^{-1/4}\sigma, \qquad (B17)$$

so that both conditions (B16) are satisfied in the limit $N \gg 1$.

We generate a large number of Monte Carlo events. For each event, we sample the positions of N sources, where N is the same for all events, according to the distribution (B8). The initial entropy density in the event is then defined by Eqs. (B1) and (B15). We then compute the corresponding energy density, $\epsilon(x)$, using the equation of state, Eq. (B9). Since the equation of state is scale invariant, the final results are independent of the normalization constant in Eq. (B15). We carry out two sets of calculations, using two different values of the speed of sound: $c_s^2 = \frac{1}{3}$ corresponding to the quark-gluon plasma at high temperature, and a value twice smaller, in order to check that the analytic results capture the dependence of fluctuation observables on c_s. The total energy, E_0, is evaluated by integrating the energy density, $E_0 \equiv \int_x \epsilon(x)$. Its cumulants (mean, variance, skewness) are finally evaluated by averaging over the ensemble of events.

Figure 4 displays our results for the relative fluctuation, the standardized skewness, and the intensive skewness, together with the perturbative results of Eqs. (B14). Agreement is not perfect, which shows that a leading-order perturbative calculation is not accurate enough even with a few hundred sources. Nevertheless, the perturbative results capture the order of magnitude and the dependence on c_s^2: In particular, Monte Carlo results confirm that a softer equation of state results in narrower fluctuations, with a larger intensive skewness.

[1] J. Adams *et al.* [STAR Collaboration], Phys. Rev. C **71**, 064906 (2005) doi:10.1103/PhysRevC.71.064906 [nucl-ex/0308033].

[2] J. Adams *et al.* [STAR Collaboration], Phys. Rev. C **72**, 044902 (2005) doi:10.1103/PhysRevC.72.044902 [nucl-ex/0504031].

[3] L. Adamczyk *et al.* [STAR Collaboration], Phys. Rev. C **87**, no. 6, 064902 (2013) doi:10.1103/PhysRevC.87.064902 [arXiv:1301.6633 [nucl-ex]].

[4] J. Adam *et al.* [STAR Collaboration], Phys. Rev. C **99**, no. 4, 044918 (2019) doi:10.1103/PhysRevC.99.044918 [arXiv:1901.00837 [nucl-ex]].

[5] B. B. Abelev *et al.* [ALICE Collaboration], Eur. Phys. J. C **74**, no. 10, 3077 (2014) doi:10.1140/epjc/s10052-014-3077-y [arXiv:1407.5530 [nucl-ex]].

[6] P. Bo?ek and W. Broniowski, Phys. Rev. C **96**, no. 1, 014904 (2017) doi:10.1103/PhysRevC.96.014904 [arXiv:1701.09105 [nucl-th]].

[7] J. E. Bernhard, J. S. Moreland and S. A. Bass, Nature Phys. **15**, no. 11, 1113 (2019). doi:10.1038/s41567-019-0611-8

[8] F. G. Gardim, G. Giacalone, M. Luzum and J. Y. Ollitrault, arXiv:2002.07008 [nucl-th].

[9] G. Giacalone, F. G. Gardim, J. Noronha-Hostler and J. Y. Ollitrault, arXiv:2004.01765 [nucl-th].

[10] J. P. Blaizot, W. Broniowski and J. Y. Ollitrault, Phys. Lett. B **738**, 166 (2014) doi:10.1016/j.physletb.2014.09.028 [arXiv:1405.3572 [nucl-th]].

[11] S. Floerchinger and U. A. Wiedemann, JHEP **1408**, 005 (2014) doi:10.1007/JHEP08(2014)005 [arXiv:1405.4393 [hep-ph]].

[12] G. Giacalone, J. Noronha-Hostler, M. Luzum and J. Y. Ollitrault, Phys. Rev. C **97**, no. 3, 034904 (2018) doi:10.1103/PhysRevC.97.034904 [arXiv:1711.08499 [nucl-th]].

[13] J. Noronha-Hostler, G. S. Denicol, J. Noronha, R. P. G. Andrade and F. Grassi, Phys. Rev. C **88**, no. 4, 044916 (2013) doi:10.1103/PhysRevC.88.044916 [arXiv:1305.1981 [nucl-th]].

[14] J. Noronha-Hostler, J. Noronha and F. Grassi, Phys. Rev. C **90**, no. 3, 034907 (2014) doi:10.1103/PhysRevC.90.034907 [arXiv:1406.3333 [nucl-th]].

[15] J. Noronha-Hostler, J. Noronha and M. Gyulassy, Phys. Rev. C **93**, no. 2, 024909 (2016) doi:10.1103/PhysRevC.93.024909 [arXiv:1508.02455 [nucl-th]].

[16] J. S. Moreland, J. E. Bernhard and S. A. Bass, Phys. Rev. C **92**, no. 1, 011901 (2015) doi:10.1103/PhysRevC.92.011901 [arXiv:1412.4708 [nucl-th]].

[17] J. E. Bernhard, J. S. Moreland, S. A. Bass, J. Liu and U. Heinz, Phys. Rev. C **94**, no. 2, 024907 (2016) doi:10.1103/PhysRevC.94.024907 [arXiv:1605.03954 [nucl-th]].

[18] J. Vredevoogd and S. Pratt, Phys. Rev. C **79**, 044915 (2009) doi:10.1103/PhysRevC.79.044915 [arXiv:0810.4325 [nucl-th]].

[19] W. van der Schee, P. Romatschke and S. Pratt, Phys. Rev. Lett. **111**, no. 22, 222302 (2013) doi:10.1103/PhysRevLett.111.222302 [arXiv:1307.2539 [nucl-th]].

[20] A. Kurkela, A. Mazeliauskas, J. F. Paquet, S. Schlichting and D. Teaney, Phys. Rev. Lett. **122**, no. 12, 122302 (2019) doi:10.1103/PhysRevLett.122.122302 [arXiv:1805.01604 [hep-ph]].

[21] P. F. Kolb, P. Huovinen, U. W. Heinz and H. Heiselberg, Phys. Lett. B **500**, 232 (2001) doi:10.1016/S0370-2693(01)00079-X [hep-ph/0012137].

[22] P. Alba, V. Mantovani Sarti, J. Noronha, J. Noronha-Hostler, P. Parotto, I. Portillo Vazquez and C. Ratti, Phys. Rev. C **98**, no. 3, 034909 (2018) doi:10.1103/PhysRevC.98.034909 [arXiv:1711.05207 [nucl-th]].

[23] S. Borsanyi, Z. Fodor, C. Hoelbling, S. D. Katz, S. Krieg and K. K. Szabo, Phys. Lett. B **730**, 99 (2014) doi:10.1016/j.physletb.2014.01.007 [arXiv:1309.5258 [hep-lat]].

[24] D. Teaney, Phys. Rev. C **68**, 034913 (2003) doi:10.1103/PhysRevC.68.034913 [nucl-th/0301099].

[25] P. Alba *et al.*, Phys. Rev. D **96**, no. 3, 034517 (2017) doi:10.1103/PhysRevD.96.034517 [arXiv:1702.01113 [hep-lat]].

[26] S. A. Bass and A. Dumitru, Phys. Rev. C **61**, 064909 (2000) doi:10.1103/PhysRevC.61.064909 [nucl-th/0001033].

[27] D. Teaney, J. Lauret and E. V. Shuryak, nucl-th/0110037.

[28] C. E. Aguiar, Y. Hama, T. Kodama and T. Osada, Nucl. Phys. A **698**, 639 (2002) doi:10.1016/S0375-9474(01)01447-6 [hep-ph/0106266].

[29] H. Holopainen, H. Niemi and K. J. Eskola, Phys. Rev. C **83**, 034901 (2011) doi:10.1103/PhysRevC.83.034901 [arXiv:1007.0368 [hep-ph]].

[30] H. Petersen, G. Y. Qin, S. A. Bass and B. Muller, Phys. Rev. C **82**, 041901 (2010) doi:10.1103/PhysRevC.82.041901 [arXiv:1008.0625 [nucl-th]].

[31] B. Schenke, S. Jeon and C. Gale, Phys. Rev. Lett. **106**, 042301 (2011) doi:10.1103/PhysRevLett.106.042301 [arXiv:1009.3244 [hep-ph]].

[32] F. Cooper and G. Frye, Phys. Rev. D **10**, 186 (1974). doi:10.1103/PhysRevD.10.186

[33] A. Mazeliauskas, S. Floerchinger, E. Grossi and D. Teaney, Eur. Phys. J. C **79**, no. 3, 284 (2019) doi:10.1140/epjc/s10052-019-6791-7 [arXiv:1809.11049 [nucl-th]].

[34] P. Bozek and W. Broniowski, Phys. Rev. C **85**, 044910 (2012) doi:10.1103/PhysRevC.85.044910 [arXiv:1203.1810 [nucl-th]].

[35] F. G. Gardim, F. Grassi, P. Ishida, M. Luzum and J. Y. Ollitrault, Phys. Rev. C **100**, no. 5, 054905 (2019) doi:10.1103/PhysRevC.100.054905 [arXiv:1906.03045 [nucl-th]].

[36] H. Grönqvist, J. P. Blaizot and J. Y. Ollitrault, Phys. Rev. C **94**, no. 3, 034905 (2016) doi:10.1103/PhysRevC.94.034905 [arXiv:1604.07230 [nucl-th]].

[37] G. Giacalone, L. Yan, J. Noronha-Hostler and J. Y. Ollitrault, Phys. Rev. C **95**, no. 1, 014913 (2017) doi:10.1103/PhysRevC.95.014913 [arXiv:1608.01823 [nucl-th]].

[38] A. M. Sirunyan *et al.* [CMS Collaboration], Phys. Lett. B **789**, 643 (2019) doi:10.1016/j.physletb.2018.11.063 [arXiv:1711.05594 [nucl-ex]].

[39] S. Acharya *et al.* [ALICE Collaboration], JHEP **1807**, 103 (2018) doi:10.1007/JHEP07(2018)103 [arXiv:1804.02944 [nucl-ex]].

[40] L. Yan and J. Y. Ollitrault, Phys. Rev. Lett. **112**, 082301 (2014) doi:10.1103/PhysRevLett.112.082301 [arXiv:1312.6555 [nucl-th]].

[41] A. M. Sirunyan *et al.* [CMS Collaboration],

Phys. Rev. C **101**, no. 1, 014912 (2020) doi:10.1103/PhysRevC.101.014912 [arXiv:1904.11519 [hep-ex]].

[42] G. Aad *et al.* [ATLAS Collaboration], Eur. Phys. J. C **79**, no. 12, 985 (2019) doi:10.1140/epjc/s10052-019-7489-6 [arXiv:1907.05176 [nucl-ex]].

[43] M. L. Miller, K. Reygers, S. J. Sanders and P. Steinberg, Ann. Rev. Nucl. Part. Sci. **57**, 205 (2007) doi:10.1146/annurev.nucl.57.090506.123020 [nucl-ex/0701025].

[44] R. S. Bhalerao, G. Giacalone and J. Y. Ollitrault, Phys. Rev. C **100**, no. 1, 014909 (2019) doi:10.1103/PhysRevC.100.014909 [arXiv:1904.10350 [nucl-th]].

[45] R. Rogly, G. Giacalone and J. Y. Ollitrault, Phys. Rev. C **98**, no. 2, 024902 (2018) doi:10.1103/PhysRevC.98.024902 [arXiv:1804.03031 [nucl-th]].

[46] F. G. Gardim, G. Giacalone, M. Luzum and J. Y. Ollitrault, Nat. Phys. (2020) doi:10.1038/s41567-020-0846-4 [arXiv:1908.09728 [nucl-th]].

[47] B. Schenke, C. Shen and D. Teaney, arXiv:2004.00690 [nucl-th].

[48] R. S. Bhalerao, G. Giacalone, P. Guerrero-Rodríguez, M. Luzum, C. Marquet and J. Y. Ollitrault, Acta Phys. Polon. B **50**, 1165 (2019) doi:10.5506/APhysPolB.50.1165 [arXiv:1903.06366 [nucl-th]].

[49] R. S. Bhalerao, M. Luzum and J. Y. Ollitrault, Phys. Rev. C **84**, 054901 (2011) doi:10.1103/PhysRevC.84.054901 [arXiv:1107.5485 [nucl-th]].

[50] A. Mazeliauskas and D. Teaney, Phys. Rev. C **91**, no. 4, 044902 (2015) doi:10.1103/PhysRevC.91.044902 [arXiv:1501.03138 [nucl-th]].

[51] F. G. Gardim, F. Grassi, P. Ishida, M. Luzum, P. S. Magalãhes and J. Noronha-Hostler, Phys. Rev. C **97**, no. 6, 064919 (2018) doi:10.1103/PhysRevC.97.064919 [arXiv:1712.03912 [nucl-th]].

[52] P. Di Francesco, M. Guilbaud, M. Luzum and J. Y. Ollitrault, Phys. Rev. C **95**, no. 4, 044911 (2017) doi:10.1103/PhysRevC.95.044911 [arXiv:1612.05634 [nucl-th]].

[53] S. S. Adler *et al.* [PHENIX Collaboration], Phys. Rev. Lett. **91**, 182301 (2003) doi:10.1103/PhysRevLett.91.182301 [nucl-ex/0305013].

[54] N. Borghini, P. M. Dinh and J. Y. Ollitrault, Phys. Rev. C **63**, 054906 (2001) doi:10.1103/PhysRevC.63.054906 [nucl-th/0007063].

[55] F. Gelis, G. Giacalone, P. Guerrero-Rodríguez, C. Marquet and J. Y. Ollitrault, arXiv:1907.10948 [nucl-th].